A Revised Diameter for the Serpent Mound Impact Crater in Southern Ohio

Keith A. Milam[1], Department of Geological Sciences, Ohio University, Athens, OH

Abstract. Previous studies of the Serpent Mound impact crater in southern Ohio have identified only two of the three important landforms associated with complex impact craters: the central peak and the surrounding graben (the latter coinciding with area beneath the crater floor). The third landform, the crater rim, was never identified. The diameter (7 to 8 km) of the area that encompasses both the central peak and ring graben was previously offered as the diameter of the crater, which was not representative of the full extent of this crater. Morphometric analysis, a reexamination of the local morphology, and delineation of structural deformation using subsurface data have provided new insight concerning the actual size of the Serpent Mound impact crater. Results suggest that the Serpent Mound impact crater is approximately 14 km in diameter and that surficial remnants of a crater rim still exist along the eastern half of the crater.

OHIO J SCI 110 (3): 34-43, 2010

INTRODUCTION

The Serpent Mound crater (centered at 39.0356° N, 83.4039° W) is the only verified impact crater in the state of Ohio (Fig. 1). It is a complex crater by type with evidence of shock metamorphism (Dietz 1960; Cohen and others 1961; Carlton and others 1998; Milam and others, 2011) required for impact crater identification (French 1998). Like all complex craters, it contains a central peak of structurally-uplifted material (Bucher 1933; Reidel 1975; Reidel and others 1982; Baranoski and others 2003). This peak of deformed Upper Ordovician to Middle Silurian-aged carbonate rock (Reidel 1975; Reidel and others 1982) is surrounded by a circular graben of Middle Silurian – Lower Mississippian sedimentary rock (Reidel 1975). Circumferential normal faults of this graben approximate the outermost boundary of the disturbed area (Fig. 1), resulting in a structure that was estimated to be 7 to 8 km in diameter (Reidel 1975).

Reidel's (1975) estimate cannot represent the total diameter of the Serpent Mound impact crater. A central peak and surrounding crater floor (that was displaced downward from normal position – i.e. a "ring graben") are only the inner parts of the overall morphology of a complex crater. Complex craters also have outer rims that are characterized by concentric, imbricated, normal faults along which the initial or transient crater rim collapsed inward following crater excavation (French 1998). This produces a series of terraces along the modified crater rim. Figure 2 shows representative examples of complex impact craters on Mars, the moon and Venus with central peaks (white arrows), crater rims (black arrows), and crater floors (between the peak and rim). While a central peak and graben have been observed at Serpent Mound (Reidel 1975; Reidel and others 1982), a rim had yet to be identified. This lack of rim identification may be related to extensive erosion of the rim, especially in the western part of the crater in the ring graben. In the crater's northwest quadrant, glacial activity has removed morphologic traces of a rim and deposited Illinoian glacial till (Reidel 1975), while in the southwest quadrant, drainage along Brush Creek has eroded into the crater interior as far as the ring graben. Along the eastern half of the crater, between the graben and the Allegheny Escarpment (Fig. 1), the landscape consists of gently rolling farmland with a paucity of bedrock exposures and no obvious topographic indication of a rim. Field investigations near the crater are limited in scope by extensive erosion, thick soil cover, and heavy vegetation in this area; therefore a new approach was needed to analyze the Serpent Mound crater. This study applies known crater morphometric relationships to model the crater diameter and uses new morphologic and subsurface data in an attempt to identify a crater rim and to constrain the diameter of the Serpent Mound impact crater.

[1]Address correspondence to Keith A. Milam, 213 Clippinger Laboratories, Athens, OH 45701. Email: milamk@ohio.edu

METHODS, MATERIALS, AND RESULTS

Morphometric Model of the Crater Diameter

The dimensions between crater landforms (e.g. central peaks, crater rims) on any solid body in the solar system exhibit specific proportional relationships that scale with the gravitation potential of the impacted body. For example, the depth of a complex crater on the moon is approximately 20 percent of the crater diameter (Pike 1977). We can use known morphometric relationships derived from the study of impact craters throughout the solar system to estimate the diameter of the Serpent Mound crater. One particularly useful morphometric relationship is one between the diameters of the central peak and the crater rim. Pike (1985) demonstrated that in smaller ($\leq$ 25 km diameter) terrestrial impact craters, the mean morphometric relationship between the base diameter of the central peak (D_{cp}) and the rim-to-rim crater diameter (D) is represented by:

$$D_{cp} = (0.23 \pm 0.03)D .$$

This relationship is comparable to those (0.17D to 0.26D) for complex impact craters on Mercury, Mars, Callisto, and Ganymede (Hale and Head 1980a and b; Pike 1988). This ratio can be used to estimate the diameter of the Serpent Mound crater, but to do so requires accurate measurement of D_{cp}. In the case of a relatively pristine martian or lunar crater, D_{cp} can be measured in cases where noticeable slope changes highlight the base of a well-defined central peak. In heavily eroded craters such as Serpent Mound, slope changes between the crater floor and central peak are not as evident. Therefore, both topographic analysis and other methods had to be employed to accurately constrain D_{cp}.

Table 1 lists several estimates of the central peak diameter for Serpent Mound and how they were derived. Estimated central peak diameters from previous work are not suitable for morphometric analysis. Reidel (1975) first estimated a D_{cp} of 4.8 km, but failed to report the methods employed. Schedl (2006) followed with an estimate of 3.65 km using the smallest circle that encompassed all exposures of Ordovician-Silurian limestone within the crater. However, this diameter does not correspond to the mapped area of uplifted Ordovician-Silurian carbonates from Reidel (1975) and incorrectly assumes that all Ordovician and Silurian strata have been uplifted above their normal positions, an idea that is not supported by geologic mapping (see Reidel and others 1982).

Additional estimates of D_{cp} were made for this study using Space Shuttle Radar Topography Mission (SRTM) data for a defined area that includes the Serpent Mound structure as identified by Reidel (1975) and the surrounding region (latitude: 38.9500° N to 39.1583° N, longitude: -83.3533° W to -83.5167° W; Fig. 3). SRTM data were collected using interferometric synthetic aperture radar as a part of Space Shuttle Endeavour's STS-99 mission in 2000. For more information on the SRTM see Rabus and others (2003). A digital elevation model (DEM) was produced for the study area (Fig. 3) using one arc second resolution NED data provided by the United States Geological Survey (seamless.usgs.gov). The DEM and topographic profiles were produced using commercially-available geospatial analysis software (ENVI). Prominent slope changes along two topographic cross sections were used to estimate D_{cp}, a method comparable to the base-to-base diameter estimates from planetary remote sensing studies (Pike 1977). NNE-SSW (A-A'in Fig. 3a) and NE-SW (B – B'in Figure 3a) profiles are shown in Fig. 4. This technique generated central peak diameters that ranged from ~4.6 to 5 km (Table 1).

Identification of prominent slope changes in the Serpent Mound crater may be unreliable due modification of the boundary between the central peak and the crater floor caused by erosion. Therefore, the same DEM was used in conjunction with a map of uplifted strata in the crater center (Reidel and others 1982) to estimate the diameter of the structurally uplifted area as a proxy for D_{cp}. Diameter estimates are listed in Table 1 and range from 3.2 to 3.9 km.

Another method of approximating D_{cp} is to measure the diameter of the area over which shatter cones are present. Previous studies [e.g. Howard and Offield 1968; Robertson 1968; Roddy 1968; Wilson and Stearns 1968] have demonstrated that parautochthonous bedrock exposures of shatter cones are confined to the central uplift of complex craters. In some cases (e.g. Sierra Madera – Howard and Offield 1968, Slate Islands – Dressler et al. 1998), the shatter-coned area closely corresponds to uplifted rocks at a crater's center. Exceptions to this correspondence exist and are affectded by rock type, where shatter cones are more distinct in fine-grained rocks compared to coarser varieties (Koeberl 2002). Rock type seems to affect the formation of shatter cones, favoring fine-grained rocks over coarser varieties (Koeberl 2002). For example, in the Wells Creek impact structure in Tennessee, shatter cones are common in the Knox Dolomite over a 1.77 km diameter area, however the diameter of the central uplift is measured at 4.8 km (Wilson and Stearns 1968). Although the area of shatter-coned bedrock may not reflect the full extent of central uplift, shatter cones are not present outside of central peak or uplift (with the exception of

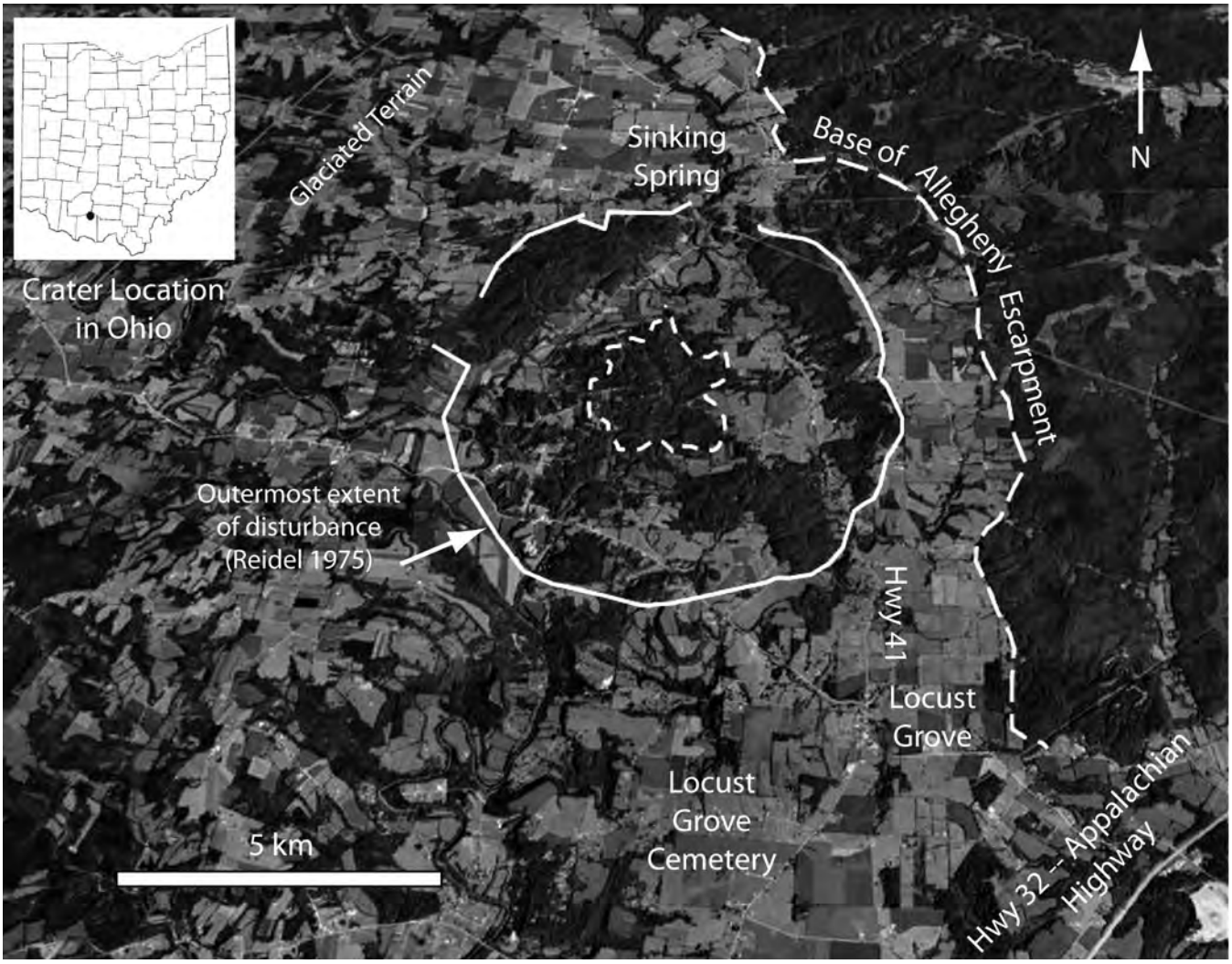

FIGURE 1. Oblique aerial view (visible image) of the Serpent Mound impact crater in southern Ohio with prominent features highlighted. The irregular dashed line in the image center highlights the approximate boundary of structurally uplifted material associated with the central peak. Aerial photo courtesy of the U.S. Department of Agriculture/Google Earth, downloaded 2010.

those present in ejected material). Therefore, the diameter of the area in which parautochthonous shatter cones are present should be considered the *minimum* diameter of a central uplift. The diameter of the area over which shatter cones are exposed at Serpent Mound [using locations from Reidel (1975) and Milam and others (2011)] is measured as 2.6 km, a diameter that is nearly half of the maximum estimate (4.6 to 5 km) using other techniques (Table 1). Also this 2.6 km estimate does not correspond to the transect diameter range (3.2 to 3.9 km) for uplifted strata at Serpent Mound and therefore may not represent the full diameter of the central peak.

Estimates of D_{cp} were used to revise and constrain the probable crater rim diameter of Serpent Mound. Substituting both the maximum and minimum estimated central peak diameters (Table 1) into the equation above yields an estimated rim-to-rim diameter ranging from 10 to 25 km, approximately 1.5 to 3 times that reported by Reidel (1975).

Morphologic Indication of a Rim?

Because morphometric analysis and modeling suggested that the diameter of the Serpent Mound impact crater must be larger than previously thought, a re-examination of the DEM for the study area was conducted to determine if there were any morphologic traces of a crater rim. Features typical in eroded complex craters include a circular ridge or series of concentric circular ridges or terraces corresponding to a modified crater rim. Circular drainage patterns can also serve to constrain the rim location. Circular drainage can develop along concentric normal faults common in collapsed complex crater rims. Figure 3a shows a one arc second SRTM-generated DEM for the Serpent Mound study area. This gray scale image depicts higher and lower elevations as brighter and darker colors respectively. The central peak and circular hills of the ring graben are evident in this view due to the relief between these landforms and the surrounding terrain. Drainage in the study area is primarily dendritic. A somewhat circular or arching pattern is located between the eastern part of the ring graben and the Allegheny Escarpment, conforming to the shape of the ring graben (outside of the dotted line in Fig. 3a). No convincingly circular drainage exists beyond this, limiting delineation of a crater rim beyond the disturbed area defined by Reidel (1975).

Higher elevations in the DEM to the east and south of the crater indicate that traces of an eroded rim may exist for Serpent Mound. Figure 3b shows the same DEM as Fig. 3a, but with elevations < 81 m above sea level (asl) excluded from view. This enhancement highlights the conspicuous circularity of the Allegheny Escarpment (also see Fig. 1) and its conformity to the shape of the disturbed area and ring graben mapped by Reidel (1975). This arc also appears to extend to the SSE of the structure in the form of a small hill (corresponding to the location of Locust Grove Cemetery in Fig. 1) approximately the same distance from the center of the crater.

TABLE 1
Estimated Cental Peak Diameters and Modeled Crater Diameters for the Serpent Mound Impact Crater

Method of Estimating D_{cp}	Estimated Central Peak Diameter, D_{cp} (km)	Estimated Rim-to-Rim Crater Diameter, D (km)
Previous Work		
maximum diameter arbitrarily defined by Reidel (1975)	4.8	18.5 - 24
smallest circle encompassing all exposures of Ordovician-Silurian limestone within the crater (Schall 2006)	3.7	14.2 - 18.5
Approximate Base-to-Base		
measured between prominent slope changes along a NE-SW transect using SRTM data	5.0	19.2 - 25
measured based on topographic breaks along a NNE-SWW transect using SRTM data	4.6	17.7 - 23
Uplifted Area		
measured diameter along NE-SW transect using Reidel and others (1982)	3.9	15 - 19.5
measured diameter along NE-SE transect using Reidel and others (1982)	3.2	12.3 - 16
Shatter-Coned Area		
measured from shatter cone locations in Reidel (1975) and Milam and others (2011)	2.6	10 - 13

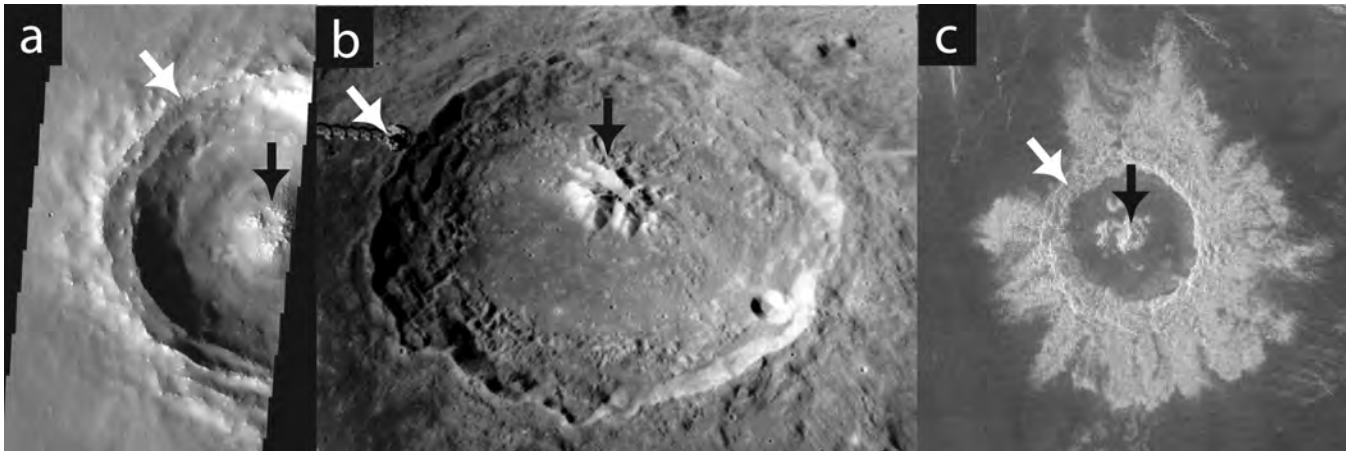

FIGURE 2. Examples of complex craters on solid bodies in the solar system: (a) Thermal Emission Imaging System (THEMIS) visible image of a unnamed complex crater near Coprates Chasma on Mars (~ 18.0°N, 294.5°E) at 17 m/pixel resolution (NASA/JPL/ASU), (b) Apollo 16 image of 110 km diameter lunar crater Theophilus centered at 11.4°S, 11.4°W (NASA), and (c) an unnamed ~40 km diameter complex crater in the Lavinia Region of Venus (NASA/JPL). Black and white arrows in all images highlight central peaks and crater rims respectively.

Eighty-two topographic cross sections were made from the center of the crater across this circular ridge (Table 2) to measure its radius. Two example cross sections are shown in Fig. 5. The center of the crater was defined at a high point in the central peak located approximately near the center of the impact crater (39.0356° N, 83.4039° W). Cross sections were produced from this center point along bearings corresponding to places where the circular ridge was present (between N 31.5 E to S 55 E and S 24 E to S 3 E) and ending at points east of the highest point of the ridge. Each radius was measured from the center point to the highest point along the top of the ridge. Radii ranged from 5.07 to 7.06 km, with a mean of 6.01 km and a 1δ standard deviation of 0.455 km. The radii values were doubled to approximate the full rim-to-rim diameter of Serpent Mound based on the assumption that the circular ridge represents vestiges of the rim for the eastern half of the impact crater. Diameters ranged from 10.1 to 14.1 km, with a mean of 12.0 km and a 1δ standard deviation of 0.904 km (Table 2). The highest points of the ridge ranged from 79.9 to 117. m asl with a mean of 104 m and a 1δ standard deviation of 10.9 km. Variations in radii and high-point elevations correspond to local drainage and therefore suggest that erosional modification has affected the morphology of this circular ridge.

The Lateral Extent of Structural Deformation

Crater morphology alone provides only circumstantial evidence for a crater rim. An examination of structural deformation beyond the interior of a complex impact crater can serve to delineate the location of the modified rim through the identification of concentric normal faults along the crater periphery. Previous geologic mapping by Reidel (1975) indicates the extent of structural deformation occurs over a roughly circular 7 to 8 km diameter area. The paucity of exposures beyond the ring graben precludes a thorough examination of the structural geology at the surface.

Subsurface data however, has provided a means of assessing the true lateral extent of structural deformation associated with the impact crater. Hundreds of well logs for oil, gas, and water wells for the study area (provided in 2010 courtesy of the Ohio Division of Geological Survey, Department of Natural Resources) were examined in search of the most identifiable geologic boundary in the Serpent Mound area. This contact is that between Middle Silurian carbonates (Peebles Dolomite, Tymochtee Formation, and Greenfield Dolomite and the fissile brown and black shales of the Upper Devonian Olentangy and Ohio Shales. Well logs for 18 townships in four counties (Table 3) were examined in the Division of Geological Survey databases. This log analysis covered the impact structure and the area centered immediately to the east and west of the Allegheny Escarpment where the Silurian-Devonian contact was most likely to still be preserved. Devonian shales have been removed by glacial activity to the west and generally dip below most well holes further to the east. Table 4 lists only those drilling logs selected for subsurface contouring based the contact between the black shales of the Upper Devonian and the gray or white carbonates of the Middle Silurian being clearly identifiable and which had reported geographic coordinates or street addresses. In the 17 instances where street addresses were the only location information available, latitude-longitude coordinates were estimated from the DEM from the center of the property. Contact elevations were determined by subtracting the depth to the contact from the well top elevations provided in each log. In instances where geographic locations had to be approximated, well top elevations were collected from the DEM of the study area. In addition, this study used seven locations from the Reidel (1975) geologic map that were suitable for constraining the contact within the crater and five stations collected for this study by a Global Positioning System (GPS) receiver (horizontal and vertical errors of $\leq \pm 3.7$ m and ± 3.048 m respectively) in the Brush Creek township of Highland County where the contact is well exposed (Table 3).

These data points were input into a contour surface modeling program (3DField, by Vladimir Galouchko) to produce a kriged contour map of the base of the Devonian in and surrounding the Serpent Mound impact crater. Figure 6a shows the contour map based on well data and surface observations from this study and

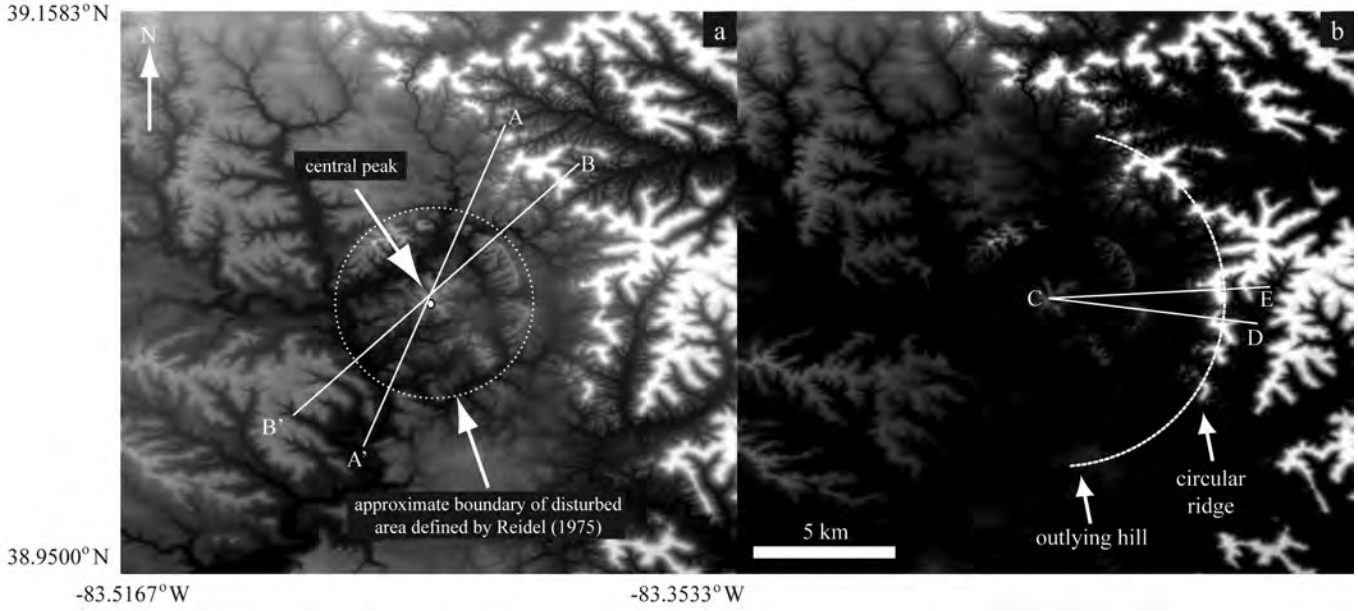

Figure 3. Digital elevation models for the Serpent Mound impact crater and surrounding areas. Higher and lower elevations are shown as brighter and darker grayscale hues respectively in both images. (a) DEM highlighting the central peak and the dashed line indicates the approximate extent of structural deformation as defined by Reidel (1975), also see Fig. 1. (b) DEM showing only elevations above 81 m to highlight the circular eastern ridge and outlying southern hill (corresponding to Locust Grove Cemetery – see Fig. 1) which form the arc highlighted with a dashed line.

Table 2

Radii measurements from the center point of the Serpent Mound impact crater (39.0356°N, 83.4039°W) to the circular eastern ridge and corresponding diameter models. Bold numbers correspond to cross sections in Figure 5.

Profile #	From Center Point To ...	Ending elevation (m)	Radius (km)	Diameter (km)	Profile #	From Center Point To ...	Ending elevation (m)	Radius (km)	Diameter (km)
1	39.0850°N, 83.3731°W	113.80	6.1095	12.219	32	39.0653°N, 83.3481°W	110.03	5.8629	11.726
2	39.0847°N, 83.3725°W	113.34	6.1116	12.223	33	39.0644°N, 83.3478°W	109.69	5.8299	11.660
3	39.0844°N, 83.3719°W	111.84	6.0840	12.168	34	39.0664°N, 83.3417°W	108.23	6.3727	12.745
4	39.0844°N, 83.3711°W	112.37	6.1250	12.250	35	39.0656°N, 83.3408°W	107.87	6.3872	12.774
5	39.0842°N, 83.3703°W	113.57	6.1373	12.275	36	39.0628°N, 83.3350°W	117.19	6.6934	13.387
6	39.0842°N, 83.3692°W	114.02	6.1989	12.398	37	39.0600°N, 83.3400°W	107.74	6.1574	12.315
7	39.0839°N, 83.3683°W	113.99	6.1998	12.400	38	39.0594°N, 83.3389°W	100.52	6.2214	12.443
8	39.0833°N, 83.3678°W	114.68	6.1767	12.353	39	39.0603°N, 83.3328°W	109.82	6.7409	13.482
9	39.0836°N, 83.3664°W	115.07	6.2518	12.504	40	39.0597°N, 83.3317°W	113.26	6.8215	13.643
10	39.0814°N, 83.3669°W	115.24	6.0168	12.034	41	39.0594°N, 83.3294°W	112.53	6.9586	13.917
11	39.0803°N, 83.3669°W	114.20	5.9064	11.813	42	39.0589°N, 83.3281°W	117.16	7.0639	14.128
12	39.0797°N, 83.3664°W	112.46	5.8877	11.775	43	39.0433°N, 83.3449°W	84.79	5.2611	10.522
13	39.0814°N, 83.3636°W	110.55	6.1689	12.338	44	39.0411°N, 83.3340°W	84.87	5.0661	10.132
14	39.0811°N, 83.3628°W	109.83	6.2042	12.408	45	39.0392°N, 83.0392°W	83.74	5.2342	10.468
15	39.0808°N, 83.3617°W	110.51	6.2156	12.431	**46**	39.3378°N, 83.3436°W	83.80	5.2502	10.500
16	39.0806°N, 83.3611°W	111.97	6.2387	12.477	47	39.0361°N, 83.3425°W	83.68	5.3276	10.655
17	39.0800°N, 83.3603°W	111.61	6.2256	12.451	48	39.0353°N, 83.3425°W	83.41	5.3151	10.630
18	39.0794°N, 83.3597°W	109.25	6.2015	12.403	49	39.0336°N, 83.3428°W	83.74	5.2954	10.591
19	39.0789°N, 83.3592°W	107.71	6.1832	12.366	50	39.0319°N, 83.3428°W	82.25	5.3062	10.612
20	39.0781°N, 83.3589°W	108.86	6.1268	12.254	51	39.0300°N, 83.3436°W	81.70	5.2671	10.534
21	39.0775°N, 83.3583°W	110.61	6.1027	12.205	52	39.0286°N, 83.3447°W	81.88	5.1781	10.356
22	39.0769°N, 83.3575°W	111.37	6.1030	12.206	53	39.02722°N, 83.3453°W	79.93	5.1700	10.340
23	39.0761°N, 83.3569°W	111.89	6.0853	12.171	**54**	39.0258°N, 83.3447°W	81.79	5.2320	10.464
24	39.0761°N, 83.3556°W	109.72	6.1552	12.310	55	39.02389°N, 83.3414°W	105.11	5.5605	11.121
25	39.0753°N, 83.3550°W	102.19	6.1211	12.242	56	39.0225°N, 83.3408°W	91.94	5.6446	11.289
26	39.0711°N, 83.3586°W	97.78	6.1230	12.248	57	39.0225°N, 83.3406°W	104.07	5.6834	11.367
27	39.0683°N, 83.3522°W	105.58	5.7759	11.552	58	39.0208°N, 83.3397°W	104.04	5.7867	11.573
28	39.0675°N, 83.3517°W	110.45	5.7370	11.474	59	39.01806°N, 83.3411°W	107.87	5.7721	11.544
29	39.0669°N, 83.3511°W	110.54	5.7561	11.512	60	39.0169°N, 83.3428°W	110.59	5.6802	11.360
30	39.0664°N, 83.3500°W	107.76	5.7960	11.592	61	39.0156°N, 83.3436°W	110.23	5.6656	11.331
31	39.0658°N, 83.3489°W	109.39	5.8387	11.677	62	39.0133°N, 83.3425°W	108.82	5.8598	11.720

Table 2 (cont.)

Radii measurements from the center point of the Serpent Mound impact crater (39.0356°N, 83.4039°W) to the circular eastern ridge and corresponding diameter models. Bold numbers correspond to cross sections in Figure 5.

Profile #	From Center Point To ...	Ending elevation (m)	Radius (km)	Diameter (km)	Profile #	From Center Point To ...	Ending elevation (m)	Radius (km)	Diameter (km)
63	39.0119°N, 83.3431°W	108.95	5.8872	11.774	75	38.9786°N, 83.3881°W	100.56	6.4717	12.943
64	39.0111°N, 83.3525°W	108.99	5.2116	10.423	76	38.9808°N, 83.3881°W	87.95	6.3365	12.673
65	39.0092°N, 83.3517°W	96.89	5.3877	10.775	77	38.9803°N, 83.3914°W	108.92	6.2319	12.464
66	38.0053°N, 83.3483°W	108.53	5.8693	11.739	78	38.9789°N, 83.3931°W	109.85	6.3151	12.630
67	39.0033°N, 83.3481°W	106.80	6.0235	12.047	79	38.9772°N, 83.3942°W	109.84	6.5156	13.031
68	39.0011°N, 83.3483°W	108.06	6.1449	12.290	80	38.9769°N, 83.3961°W	110.15	6.5113	13.023
69	38.9994°N, 83.3492°W	96.05	6.2058	12.412	81	38.9767°N, 83.3978°W	109.73	6.5595	13.119
70	38.9981°N, 83.35°W	83.12	6.2930	12.586	82	38.9772°N, 83.3997°W	110.46	6.4871	12.974
71	38.9794°N, 83.3792°W	88.02	6.5871	13.174	average		104.14	6.0087	12.017
72	38.9794°N, 83.3811°W	95.16	6.5233	13.047	maximum		117.19	7.0639	14.128
73	38.9781°N, 83.3842°W	104.56	6.5934	13.187	minimum		79.93	5.0661	10.132
74	38.9783°N, 83.3864°W	102.38	6.5312	13.062	stdev		10.851	0.45499	0.90442

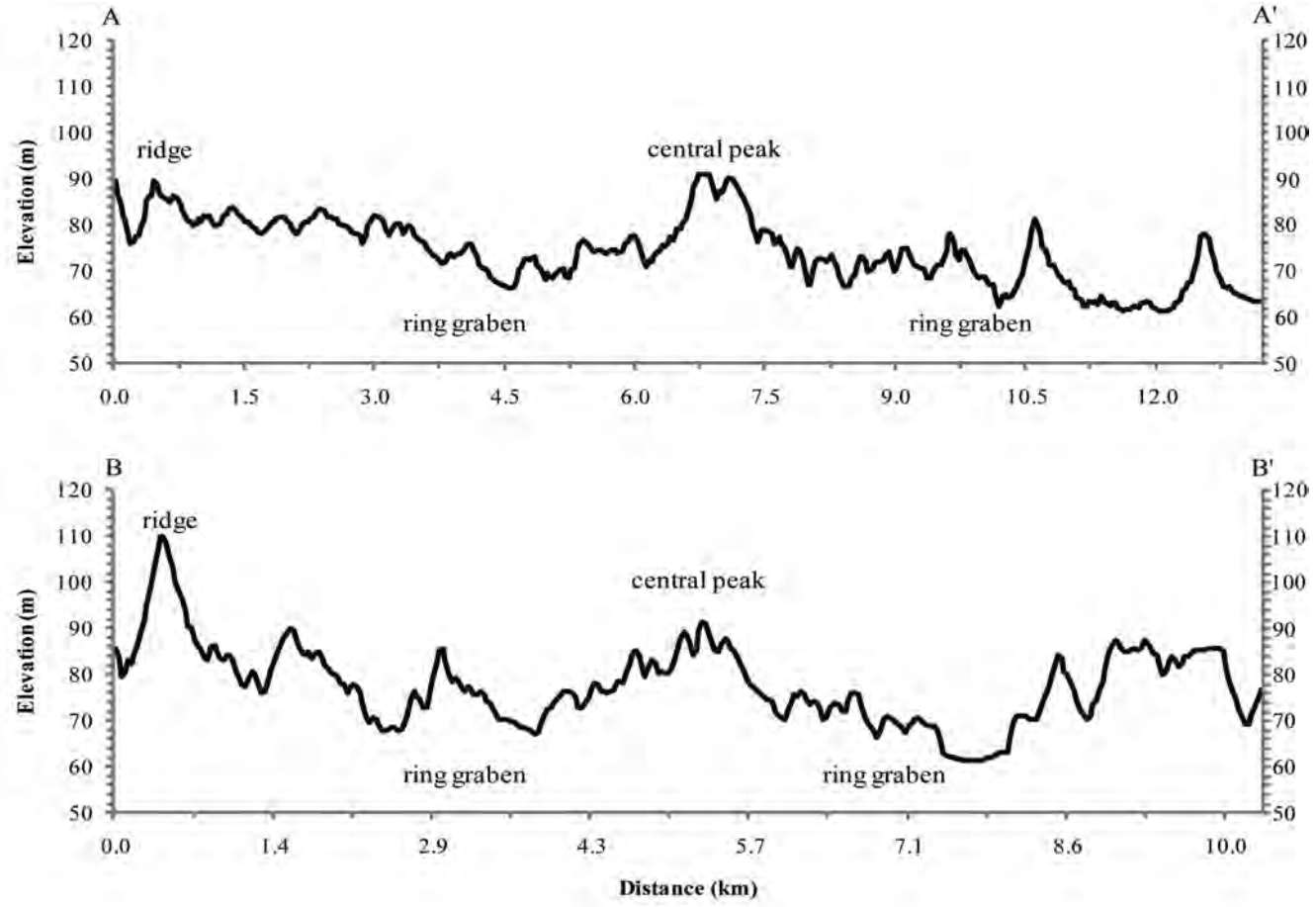

Figure 4. Topographic profiles along a NE-SW bearing (A to A'shown in Fig. 3a), W and NNE-SSW bearing (B to B' shown in Fig. 3a) with major landforms labeled. Profiles A – A' and B – B' have vertical exaggerations of 59x and 36x, respectively.

from Reidel (1975), clearly showing a circular anomaly centered at approximately 39.035° N, -83.398° W. Here the base of the Devonian is up to 58 m lower than the surrounding region and deviates from the eastward regional dip angle and direction (0.08 to 0.09° E). When data from within approximately 7 km of the crater center (39.0356° N, 83.4039° W) are removed (Fig. 6b), the regional dip is restored across the study area, highlighting the influence of the impact crater on this important contact in the area. It is important to note that the maximum displacement exceeds the maximum amount of relief (21.4 m) noted by Swinford (1985) along the unconformity between the Middle Silurian and Upper Devonian strata. Therefore, the extent of downward displacement of the base of the Devonian is related to the Serpent Mound impact crater and is confined to an area <14 km in diameter. The low density of well locations per unit area did not allow for discrimination of this downward displacement by faults or folds. Based on knowledge of typical structural deformation in better preserved complex craters, it is assumed that concentric normal faults facilitated this displacement.

DISCUSSION AND CONCLUSION

The three methods utilized in this study have provided independent means of constraining the probable diameter of the Serpent Mound impact crater. Morphometric analysis that involved a number of D_{cp} estimates were used to constrain the initial rim-to-rim diameter of Serpent Mound to within a range of 10 to 25 km, a value much larger than the 7 to 8 km disturbed area mapped by Reidel (1975). Re-examination of the landscape surrounding the Serpent Mound crater unveiled a semi-circular ridge approximately 5 to 7 km from the center of impact. The circularity of this ridge, its conformity to the shape of that portion of the crater defined by Reidel (1975), and extension of the ridge south of the crater away from the escarpment (as suggested by the outlying southern hill shown in Fig. 3) strongly support the hypothesis that this ridge is the eroded remnant of the crater rim in the east and southeast. Therefore, the morphology alone suggests that the Serpent Mound impact crater ranges from approximately 10 to 14 km in diameter, a value well within the constraints modeled using the known morphometric relationship of $D_{cp} = (0.23 \pm 0.03)D$ from Pike (1985). The 10 to14 km diameter also coincides with the lateral extent of structural deformation (<14 km diameter) as indicated by subsurface contouring. The consistency of modeled crater

TABLE 3
Area over which well log databases were searched.

County	Townships
Adams	Bratton, Brush Creek, Franklin, Green, Jefferson and Meigs
Highland	Brush Creek, Marshall and Paint
Pike	Camp Creek, Mifflin, Perry and Sunfish
Scioto	Brush Creek, Morgan, Nile, Rarden and Union

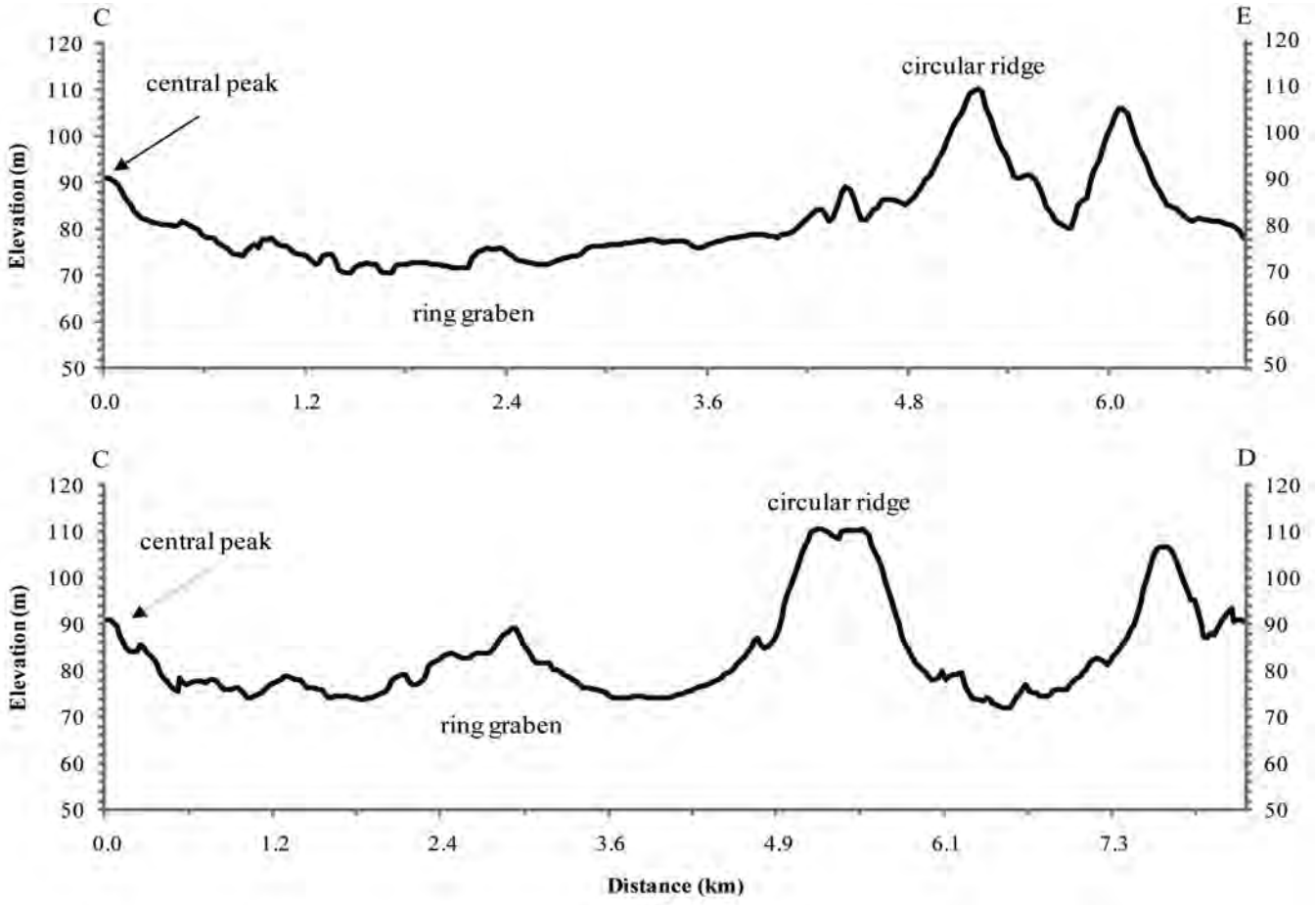

FIGURE 5. Topographic profiles from the central peak across the circular eastern ridge. Profile starting and ending points are shown in Fig. 3b. Profiles C – D and C – E have vertical exaggerations of 30x and 37x and correspond to profiles 46 and 54 on Table 2, respectively.

TABLE 4
Well Log and Surface Contact Elevations Between the Middle Silurian and Upper Devonian

Well Log No.[1]	N Lat. (dec. deg.)	W Long. (dec. deg.)	Depth to Contact (m)	Well Top Elev. (m)	Contact Elev. (m)
		Adams County -- Bratton Township			
490656*	39.037621	-83.423908	-21	213	192
[2]*	39.055332	-83.433151	--	--	244
[2]*	39.040997	-83.428768	--	--	213
[2]*	39.006642	-83.400215	--	--	232
[2]*	39.022259	-83.424877	--	--	234
		Adams County -- Brush Creek Township			
731866	38.759621	-83.440705	-14	276	263
882152	38.732480	-83.390560	-31	247	216
50864	38.768078	-83.422150	- 7	262	255
564351	38.735173	-83.407130	-22	252	231
		Adams County -- Franklin Township			
823872*	39.034400	-83.363360	-27	251	223
645876	39.021470	-83.328170	-13	240	226
936392	39.024320	-83.329350	-26	239	213
792430	38.976813	-83.310521	-22	258	236
915855	38.966101	-83.298344	-32	233	201
859263*	39.035420	-83.367830	-12	249	238
457536	38.953475	-83.328227	-10	212	202
595786	38.955100	-83.338730	- 8	217	208
792408	38.955437	-83.318668	-14	233	219
727858	38.959483	-83.297795	-12	213	201
[2]*	39.017487	-83.379205	--	--	228
[3]	39.007339	-83.342397	--	--	235
[3]	39.003491	-83.336798	--	--	226
[3]	38.990373	-83.332431	--	--	220
[3]	38.975642	-83.338685	--	--	219
[3]	38.972905	-83.342544	--	--	225
		Adams County -- Jefferson Township			
339167	38.828948	-83.278804	-85	603	158
		Adams County -- Meigs Township			
792401	38.854233	-83.326814	-27	206	179
859247	38.850020	-83.334580	-18	222	203
859247	38.851020	-83.33376	-27	219	192
679164	38.866453	-83.399843	-16	261	244
34001200090000	38.894120	-83.363251	-114	351	237
		Highland County -- Brush Creek Township			
708827	39.116487	-83.424876	- 8	298	290
703644	39.178400	-83.374900	-17	295	278
181286	39.142737	-83.413007	-18	299	281
772857	39.153400	-83.407800	-27	311	284
[2]*	39.059137	-83.387968	--	--	219
[2]*	39.058570	-83.409474	--	--	237
		Highland County -- Paint Township			
363918	39.227044	-83.366663	-17	277	260
181272	39.186526	-83.358642	-44	300	257
		Pike County -- Benton Township			
34131200200000	39.08383	-83.181917	-43	200	157
		Pike County -- Mifflin Township			
901484	39.121410	-83.319130	- 9	237	228
647868	39.121477	-83.318640	- 6	240	233
837062	39.142756	-83.336133	-17	293	276
395214	39.117129	-83.313623	-17	244	227
457530	39.121477	-83.318640	- 8	240	231
645893	39.113687	-83.314747	-24	240	215
746248	39.068998	-83.298673	- 5	219	214
647889	39.078341	-83.294456	- 8	218	210
437243	39.078318	-83.294176	-13	214	201
457527	39.070355	-83.296747	-13	225	212
457527	39.107703	-83.310326	- 7	226	219
668466	39.110949	-83.267387	-23	213	190
756836	39.126459	-83.275469	-30	228	198
352284	39.056800	-83.357633	- 5	257	251
738799	39.092489	-83.365588	-13	244	231
882127	39.129200	-83.367497	-23	289	266
437209	39.073704	-83.379533	-30	298	268

TABLE 4 (cont.)
Well Log and Surface Contact Elevations Between the Middle Silurian and Upper Devonian

Well Log No.[1]	N Lat. (dec. deg.)	W Long. (dec. deg.)	Depth to Contact (m)	Well Top Elev. (m)	Contact Elev. (m)
34131200400000	39.07059	-83.243072	-183	361	178
		Pike County -- Perry Township			
42007	39.139279	-83.354847	-24	274	250
684451	39.114383	-83.357097	- 5	256	252
341316001800	39.185399	-83.270157	-98	353	255
		Scioto County -- Brush Creek Township			
34145201950000	38.852038	-83.2280 4	-46	185	139

[1]well log numbers from the Ohio Division of the Geological Survey's oil and gas interactive map at: http://www.dnr.state.oh/Website/Geosurvey/oilgas/viewer.htm or the Ohio Division of Water's water well database at: http://dnr.ohio.gov/water/maptechs/wellogs/appNEW/

[2]selectedvalues from Reidel (1975)

[3]mapped for this study; GPS coordinates from handheld GPS Receiver with horizontal and vertical errors of <+3.7 m and + 3.048 m, respectively

* = waypoints removed from Figure 6a to produce Figure 6b

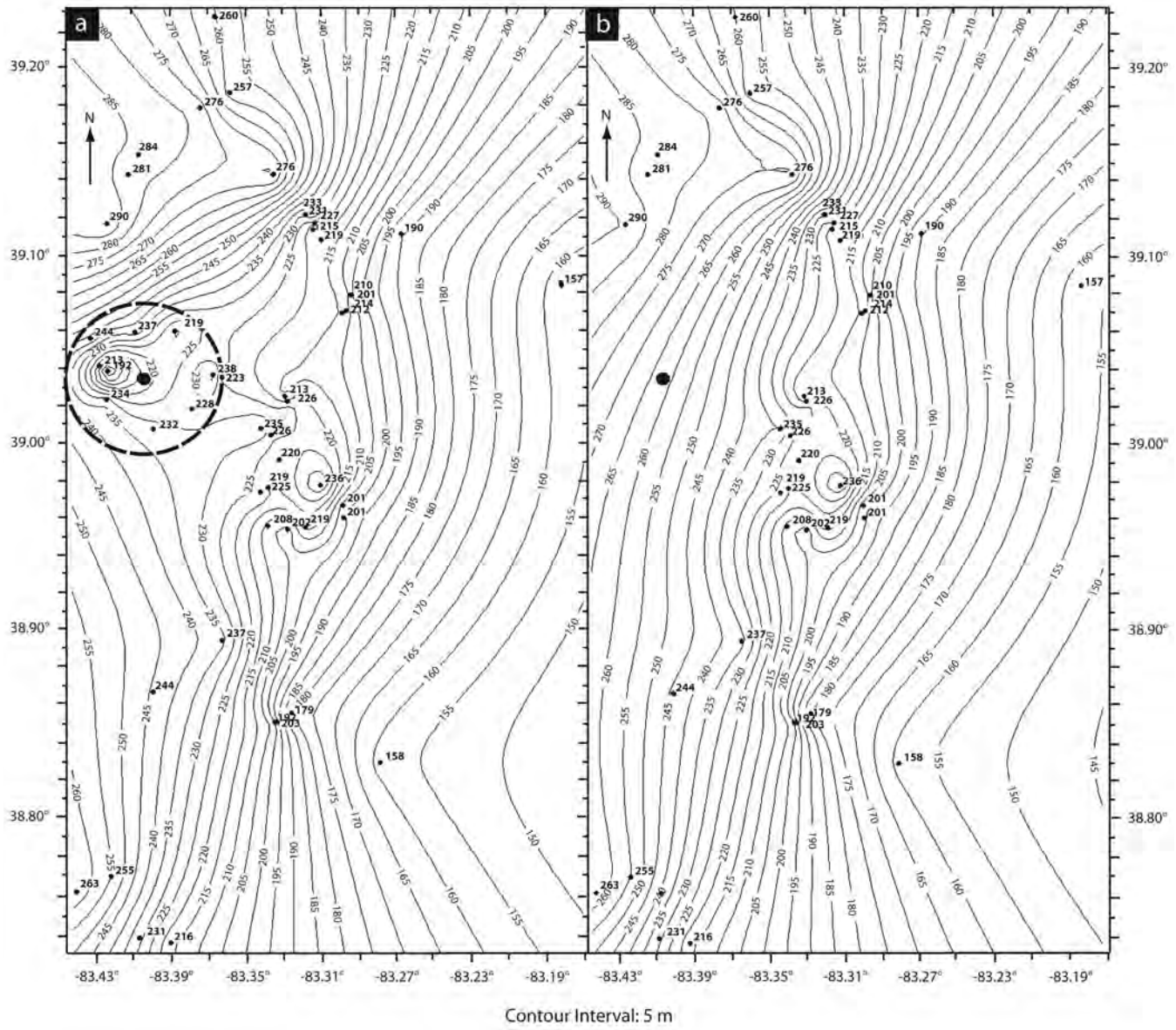

FIGURE 6. Contour maps showing the Middle Silurian – Upper Devonian (unconformable) contact in southern Ohio: (a) with data points from within the Serpent Mound crater included and (b) excluding data from within a 7 km radius of the crater center (dashed circle). The large black dot centered near 39.035° and -83.398° is the approximate center of the Serpent Mound impact crater.

diameter ranges using multiple techniques, the circularity of the eastern ridge and its conformity to the interior portions of the crater, and the lateral extent and circularity of structural deformation all suggest that the maximum diameter of the Serpent Mound impact crater is approximately 14 km and that the circular ridge east of the disturbed area as defined by Reidel (1975) represents the eroded remnant of the crater rim.

Acknowledgements. The author wishes to acknowledge Barry Duncan from the University of Little Rock in Arkansas and Lee Johnson from the Department of Geological Sciences at Ohio University for their assistance collecting data in the field. The author also wishes to thank the Ohio Division of Natural Resources Division of Geological Survey and Division of Water for access to gas, oil, and water well logs and two anonymous reviewers and my planetary geology students for their comments which improved the overall quality of this manuscript.

LITERATURE CITED

Baranoski MT, Schumacher GA, Watts DR, Carlton RW, El-Saiti BM. 2003. Subsurface geology of the Serpent Mound disturbance, Adams, Highlands, and Pike Counties, Ohio. *Report of Investigations No. 146*. Ohio Division of Geological Survey. Columbus, Ohio. 60 p.

Bucher WH. 1933. Über eine typische kryptovulaknische Störung im südlichen Ohio: *Geologicsche Rundschau* 23: 65-80.

Carlton RW, Koeberl C, Baranoski MT, Schumacher GA. 1998. Discovery of microscopic evidence for shock metamorphism at the Serpent Mound structure, south-central Ohio: confirmation of an origin by impact. *Earth and Planetary Science Letters* 162: 177-185.

Cohen AJ, Bunch TE, Reid AM. 1961. Coesite discoveries establish cryptovolcanics as fossil meteorite craters. *Science* 134(3490): 1624-1625.

Dietz RS. 1960. Meteorite impact suggested by shatter cones in rock, *Science* 131(3416): 1781-1784.

Dressler BO, Sharpton VL, Schuraytz BC. 1998. Shock metamorphism and shock barometry at a complex impact structure: Slate Islands, Canada. *Contrib. Mineral. Petrol.* 130: 275-287.

French BM. 1998. Traces of Catastrophe: A Handbook of Shock-Metamorphic Effects in Terrestrial Meteorite Impact Structures. *LPI Contribution No. 954*. Lunar and Planetary Institute, Houston, Texas.

Hale W and Head JW. 1980a. Central peaks in mercurian craters: Comparisons to the Moon. Proc Lunar Planet Sci Conf 11th: 2191 – 2205.

Hale W and Head JW. 1980b. Crater central peaks on the Moon, Mercury, and Earth. Reports on the Planetary Geology Program, NASA Technical Memorandum 82385: 131 – 133.

Howard KA and Offield TW. 1968. Shatter cones at Sierra Madera, Texas. *Science* 162 (3850): 261 – 265.

Koeberl C. 2002. Mineralogical and geochemical aspects of impact craters. Mineralogical Magazine 66(5): 745-768.

Milam KA, Gabreski C, Baranoski M, and Miller DW. (in review). Evidence of timing of the Serpent Mound impact event from shatter cones. *Ohio J Sci*.

Pike RJ. 1977. Size-dependence in the shape of fresh impact craters on the Moon In Roddy DJ, Pepin RO, and Merrill RB editors, Impact and explosion cratering. Pergamon Press, NY: 489 – 509.

Pike RJ. 1985. Some morphologic systematic of complex impact structures. *Meteoritics* 20(1): 49-68.

Pike RJ. 1988. Geomorphology of impact craters on Mercury. In Vilas F and others editors, Mercury. University of Arizona Press, Tuscon: 165 – 273.

Rabus B, Eineder M, Roth A, and Bamler R. 2003. The shuttle radar topography mission – a new class of digital elevation models acquired by spaceborne radar. *ISPRS Journal of Photogrammetry & Remote Sensing* 57: 241-262.

Reidel SP. 1975. Bedrock geology of the Serpent Mound cryptoexplosion structure, Adams, Highlands, and Pike Counties, Ohio, *Ohio Division of Geological Survey Report of Investigations No. 95*, Ohio Division of Geological Survey, map with text.

Reidel SP, Koucky, FL, Stryker, JR. 1982. The Serpent Mound disturbance, Southwest Ohio. *American Journal of Science* 282: 1343-1377.

Robertson PB. 1968. La Malbaie structure, Quebec – A Palaeozoic meteorite impact site: Meteoritics 4: 89 – 112.

Roddy DJ. 1968. The Flynn Creek Crater, Tennessee. In French BM and Short NM editors, Shock Metamorphism of Natural Materials, Mono Book Corp., Baltimore, MD: 291 – 322.

Schedl A. 2006. Applications of twin analysis to studying meteorite impact structures. EPSL 244: 530-540.

Swinford EM. 1985. Geology of the Peebles quadrangle, Adams County, Ohio. Ohio J of Sci 85(5): 218-230.

Wilson CW Jr and Stearns RG. 1968. Geology of the Wells Creek Structure, Tennessee. Bulletin 68, Tennessee Division of Geology, 236 p. with maps.